

Comprehensive analyses reveal TKI-induced remodeling of the tumor immune microenvironment in EGFR/ALK-positive non-small-cell lung cancer

Yisheng Fang^{a*}, Yuanyuan Wang^{a*}, Dongqiang Zeng^{a*}, Shimeng Zhi^a, Tingting Shu^a, Na Huang^a, Siting Zheng^a, Jianhua Wu^a, Yantan Liu^a, Genjie Huang^a, Yichen Xue^a, Jianping Bin^b, Yulin Liao^b, Min Shi^a, and Wangjun Liao^a 

^aDepartment of Oncology, Nanfang Hospital, Southern Medical University, Guangzhou, Guangdong, China; ^bDepartment of Cardiology, Nanfang Hospital, Southern Medical University, Guangzhou, Guangdong, China

ABSTRACT

Tyrosine kinase inhibitors (TKI) play a pivotal role in the treatment of non-small-cell lung cancer (NSCLC) with mutations in epidermal growth factor receptor (EGFR) and rearrangements in anaplastic lymphoma kinase (ALK). However, the influences of TKIs on the tumor immune microenvironment (TIM), especially dynamic changes of responders, have not yet been fully elucidated. Therefore, RNA sequencing and whole-exome sequencing were performed on EGFR/ALK-positive NSCLC samples before and after TKI treatment. In combination with neoantigen and mutational-load estimations, xCell and single-sample gene set enrichment analysis (ssGSEA) were used to assess tumor immune-cell infiltration and activity. Furthermore, weighted-gene correlation network analysis and the bottleneck method were used to identify the hub genes that affected treatment-related immune responses. We found that TKI treatment remodeled the TIM in treatment-responsive samples. Profound increases in the rate of anti-tumor cell infiltration and cytotoxicity was observed following TKI treatment, while antigen presentation was limited in ALK-rearranged samples. However, no significant change in anti-tumor cell infiltration or cytotoxicity was found between pre-treatment and post-progression samples. Subsequently, we found that neurofilament heavy (NEFH) mutations were enriched in samples after TKI treatment and were associated with reduced neutrophil infiltration. The cytotoxicity of EGFR-mutant NSCLCs with co-driver TP53 mutation and ALK-rearranged samples with wild-type TP53 seems to be more easily induced by TKI. Finally, the immune-associated score generated by hub genes was positively correlated with immune infiltration, immune activation, and a favorable prognosis. In conclusion, the dynamic changes in the TIM provide clues to drug selection and timing for TKI-immunotherapy combinations.

ARTICLE HISTORY

Received 28 January 2021
Revised 28 June 2021
Accepted 28 June 2021

KEYWORDS

Tumor immune microenvironment; non-small-cell lung cancer; EGFR mutation; ALK rearrangement; tyrosine kinase inhibitors

Introduction

Lung cancer is the leading cause of cancer-related death worldwide, and non-small-cell lung cancer (NSCLC) is the major histological subtype of lung cancer.¹ Nearly two-thirds of NSCLC patients have carcinogenic driver mutations, approximately half of which have treatable target lesions. These expand the scope of treatment options and may help improve survival and safety over conventional chemotherapy.² At present, most of the targetable oncogenic mutations in receptor tyrosine kinases occur in lung adenocarcinomas (ADCs). These include epidermal growth factor receptor (EGFR) mutations and anaplastic lymphoma kinase (ALK) rearrangements.³

Although the therapeutic effects of tyrosine kinases inhibitors (TKIs) have improved the prognosis of NSCLC patients, the responses to TKIs are usually incomplete and temporary.² There has been strong interest in determining whether immune-checkpoint inhibitors may produce more complete and longer-term efficacious responses in NSCLC patients. However, findings on the efficacies of immune-checkpoint inhibitors either after TKI treatments or in combination with TKI treatment have been disappointing.^{4,5} Several explanations for

these poor responses to immunotherapy in NSCLC patients harboring EGFR mutations or ALK rearrangements have been proposed – such as variable programmed death-ligand 1 (PD-L1) expression,⁶ low mutational load, and an inactive tumor immune microenvironment (TIM) characterized by a lack of infiltration of cytotoxic T cells^{4,7} – all of which may negatively affect responses to PD-1/PD-L1 inhibitors. In addition, TKIs may inhibit the expression of PD-L1 up-regulated by EGFR or ALK activation,^{8,9} thus indicating that TKIs and anti-PD-1 antibody may have a similar effect on blocking the interaction between PD-1 and PD-L1, but not a synergistic effect.^{10,11} Therefore, there is a need to further elucidate the effects of TKI treatments on the function of the immune system. Previous studies showed that ALK inhibitor crizotinib and anti-EGFR monoclonal antibody cetuximab induce immunogenic cell death in NSCLC and are linked to increased T-lymphocyte infiltration.^{12,13} However, evidence has suggested that EGFR-TKIs decrease T-cell infiltration in post-TKI-resistant samples with EGFR mutations¹⁴ and that there is no significant difference in the abundance of CD8-positive (CD8+) T cells between naïve-treatment and post-TKI-resistant mouse

CONTACT Wangjun Liao  nfyliowj@163.com  Department of Oncology, Nanfang Hospital, Southern Medical University, 1838 North Guangzhou Avenue, Guangzhou, Guangdong 510515, China

*These authors contributed equally to this work.

 Supplemental data for this article can be accessed on the [publisher's website](#).

© 2021 The Author(s). Published with license by Taylor & Francis Group, LLC.

This is an Open Access article distributed under the terms of the Creative Commons Attribution-NonCommercial License (<http://creativecommons.org/licenses/by-nc/4.0/>), which permits unrestricted non-commercial use, distribution, and reproduction in any medium, provided the original work is properly cited.

samples with ALK fusion.¹⁵ Although there are a limited number of studies on TKI-induced TIM reprogramming of TKI-resistant samples, the immunological effects of TKIs in treatment-responsive patients remain widely unknown.

Herein, using the whole-exome sequencing (WES) and RNA sequencing (RNA-seq) of the biopsies of pre-TKI and post-TKI responders, we present results assessing TKI-induced TIM remodeling and findings regarding differential patterns of immune responses between EGFR-mutant and ALK-rearranged samples via several methods, such as computing the signature score of immune cells and tumor-neoantigen estimation. We also analyzed and compared our data with public datasets to identify immune-related genes underlying TKI-induced dynamic changes of the TIM in response to TKI treatments.

Materials and methods

Data availability

Our ADC datasets generated and analyzed during the current study are not publicly available but are available from the corresponding author on reasonable request. Data from three publicly available datasets were incorporated into our study. TCGA level three RNA-seq data and clinical information from patients were acquired from the UCSC Xena website (<https://xenabrowser.net/>). Additionally, microarray data from 34 lung cancer samples with EGFR mutations from the GSE11969 dataset were downloaded from the Gene Expression Omnibus (GEO) (<http://www.ncbi.nlm.nih.gov/geo>). RNA expression data of paired pre- and post-TKI-resistant samples were available for the Osimertinib-treated cohort.¹⁶

Patients

We enrolled 23 patients with histologically confirmed EGFR mutations or ALK rearrangements in advanced lung ADCs as defined by the American Joint Committee on Cancer guidelines. Fifteen paired pre- and post-TKI samples with EGFR mutations and eight paired ALK-rearranged tissues were obtained from patients undergoing TKI treatments. With the help of computed tomography (CT) and the Response Evaluation Criteria in Solid Tumors (RECIST 1.1),¹⁷ three post-treatment samples were identified as progressive disease (PD), and the other 20 post-treatment samples were defined as partial response (PR). In total, 45 samples (including three samples from P3 patient and four samples from P4 patient) were obtained for RNA-seq analysis, and 42 samples were used for WES analysis. Patient information is summarized in Supplementary Table S1. This study was approved by the ethics committee of NangFang Hospital (NFEC-2019-265), and informed consent was obtained from all patients.

RNA sequencing (RNA-seq)

Total RNA from fresh frozen tissues was extracted with Trizol according to the manufacturer's recommendations. Sequencing libraries were generated using a KAPA Stranded RNA-Seq Kit (KAPA, USA) following the manufacturer's

instructions, and index codes were added to attribute sequences to each sample. Libraries were pooled and paired-end sequencing (2 × 150 bp reads) was performed on an Illumina X-ten PE150 platform.

Whole-exome sequencing (WES)

Fresh frozen tissues from tumor samples were used for genomic DNA extraction via a DNeasy Blood and Tissue Kit (QIAGEN) following the manufacturer's instructions. Peripheral blood DNA extracted from individual patients was used for germline exome sequencing. Extracted tumor-genomic DNA was fragmented into 300–350 bp by sonication (Covaris, Woburn, MA). Sequencing libraries were prepared with a KAPA Hyper Prep kit (KAPA Biosystems) with optimized protocols. Libraries were then subjected to PCR amplification and purification before targeted enrichment. The enriched libraries were sequenced on HiSeq 4000 NGS platforms (Illumina) to cover depths at 200x.

Further analysis of RNA-seq data

Differential gene expression analysis was conducted using DESeq2 between pre-treatment and post-treatment samples. Gene Ontology (GO) enrichment analysis of differentially expressed genes (DEGs; adjusted *p*-value < 0.05) was subsequently performed by using the R package, “clusterProfiler”.¹⁸ Gene set enrichment analysis (GSEA) was then performed on all pre-ranked genes, and enrichment scores were generated for Kyoto Encyclopedia of Genes and Genomes (KEGG) pathways. GO terms and GSEA enrichment scores with false discovery rates (FDRs) less than 0.05 were considered to be significantly enriched. Single-sample GSEA (ssGSEA) was used to generate infiltration scores for 16 immune cell types and cytotoxic cells for each tumor based on previously published gene sets¹⁹ using the R package, “gsva”.²⁰ Immune scores, microenvironment scores, and stroma scores were processed using xCell.²¹

Data processing of weighted-gene correlation network analysis (WGCNA) followed the Horvath Lab UCLA protocol (<https://horvath.genetics.ucla.edu/html/CoexpressionNetwork/Rpackages/WGCNA>). Then, the STRING network of genes in each color module was imported into Cytoscape 3.7, and hub genes were identified by the bottleneck method provided in the cytoHubba plugin.

Tumor purity estimation

ESTIMATE scores were calculated via the “ESTIMATE” R package, and the purity of each sample was evaluated using the formula described by Yoshihara et al.²²

Tumor-neoantigen estimation

We used a QBRC pipeline for neoantigen-calling with parameters that were set according to recommended values (<https://github.com/tianshilu/QBRC-Neoantigen-Pipeline>).

Statistical analysis

All statistical tests were performed using R software, version 3.6.3. Data are expressed as mean \pm standard deviation (SD). Fisher's exact tests were used for categorical data when appropriate. For comparisons of two groups, statistical significance was estimated via Student's *t*-tests. Pearson's correlation and Spearman's rank correlation coefficient was used to evaluate the correlation between two parameters when appropriate. Log-rank tests, Kaplan–Meier curves, and smooth HR curves for survival analysis were performed using the R package, “survival”. We used the “surv_cutpoint” function in the “survminer” package to define the cutoff value of NEFH and IAS. All heatmaps were generated by the “pheatmap” function (<https://github.com/raivokolde/pheatmap>). OncoPrint was used to visualize multiple genomic mutations and was constructed by the package, “maftools” (<https://github.com/PoisonAlien/maftools>). All *p*-values were based on a two-sided hypothesis, and a *p*-value of < 0.05 was considered to be statistically significant.

Results

Transcriptional landscape of EGFR-mutant and ALK-rearranged tissue responses to TKI treatments

We enrolled 23 advanced lung ADC patients with EGFR mutations (EGFR-m, $n = 15$) or ALK rearrangements (ALK-r, $n = 8$) who received EGFR- or ALK-TKI treatments (Supplemental Table S1). Paired analysis of pre-TKI treatment and partial-response samples was performed to explore transcriptomic changes. DEGs were screened with a criterion of an FDR $\leq 5\%$. We identified a total of 2,867 DEGs (1,442 up-regulated and 1,425 down-regulated DEGs; Figure 1(a,b); Supplementary Table S2) that were shared in EGFR-m and ALK-r patients in response to TKI treatments. GO enrichment analysis of shared up-regulated DEGs indicated that their potential functions were significantly related to immune responses, while down-regulated DEGs were enriched in processes regulating cell-cell adhesion and junctions (Figure 1(c)). Further analysis of unique DEGs in EGFR-m (2,787 DEGs) or ALK-r (1,538 DEGs) samples show that, compared with those of ALK-r samples, there were more DEGs related to biological processes involving immunity in EGFR-m samples (Figure 1(a,b,d,e)). Moreover, as determined by GSEA of KEGG-pathway gene sets, some immune-related and cell-cycle-related pathways were found to be significantly regulated by TKI treatments (Figure 1(f,g)). Collectively, the above results suggest that TKI treatments may change the tumor microenvironment of TKI responders with EGFR mutations or ALK rearrangements.

TKI treatments remodel the TIM of samples with EGFR mutations or ALK rearrangements

To further verify the impact of TKI treatments on the TIM, general immune estimation scores were generated via a gene signature-based method, xCell, which converts gene expression profiles to enrichment scores.²¹ In the EGFR-m samples, immune scores, microenvironment scores, and stroma scores were significantly increased after TKI treatment (Figure 2(a)). Similarly, immune scores and microenvironment scores were

significantly increased in ALK-r post-treatment samples (Figure 2(b)). However, no significant change was found between pre-treatment and post-progression samples (Supplementary Figure 1(a)).

Next, we performed ssGSEA to estimate the infiltration levels of 16 cell types in samples before and after TKI treatments. In addition, infiltration of cytotoxic cells was computed by genes overexpressed in CD8 + T cells, gamma-delta T cells, and natural killer (NK) cells to represent the overall anti-tumor activity,¹⁹ which was dramatically increased in response to TKI treatments (Figure 2(c)) but the difference was not statistically significant in TKI-resistant samples (Supplementary Figure 1(b)). Further exploration revealed that the enhanced anti-tumor response in EGFR-m was mainly due to the increased infiltration of CD8 + T cells, B cells, and so on; in ALK-r samples, NK CD56^{dim} cells – characterized by their nonspecific-antigen-dependent cell-killing ability²³ – may have had a greater impact on the enhanced anti-tumor response (Figure 2(c)). Moreover, the expression levels of gamma-interferon-signaling and immune-checkpoint genes (e.g., STAT5B, PDCD1, BTLA, and CD27) were up-regulated in response to TKI treatments (Figure 2(d)). However, some genes related to antigen presentation were down-regulated (e.g., CALR, CANX, and PDIA3) (Figure 2(d)), which may explain the limited T-cell infiltration in responders after ALK-TKIs treatment.²⁴ Findings from many recent preclinical and clinical studies have supported the long-standing hypothesis that tumors induce adaptive immune responses and that the antigens that drive effective T-cell response are tumor-specific mutant peptides (neoantigens), which are generated from somatically mutated genes.²⁵ Therefore, RNA-seq and WES were performed to estimate the burden of tumor neoantigens and mutations. Consistent with our previous results, the reduced tendency of neoantigens (Figure 2(e)) and mutational load (Figure 2(f)) may have induced weakened antigen presentation and subsequent limited anti-tumor responses of T cells in ALK-r samples during TKI treatments. Collectively, these findings suggest that the anti-tumor responses of immune cells in EGFR-m and ALK-r responders were enhanced after TKI treatments. EGFR-m samples were dominated by adaptive immune responses, while changes in innate immune responses of ALK-r samples may be more critical under the pressure of TKI treatments.

Somatic mutational landscape between pre-treatment and post-treatment samples

TKI resistance in patients with EGFR-m or ALK-r is mainly caused by acquired mutational changes, such as the EGFR T790M mutation¹ or ALK E1384K mutation;²⁶ however, somatic mutational changes in post-responding samples have still not been widely recognized. To this end, we investigated somatic mutations in samples before and after TKI treatments and identified that neurofilament heavy (NEFH) was mutated in multiple individuals in response to TKI treatments (Figure 3(a–c)). These two variants (p.E658_E659del and p.E658_K665del) led to the in-frame deletion of two or eight amino acids in the motif characterized by repeats of the tripeptide K-S-P, which may affect the phosphorylation and function

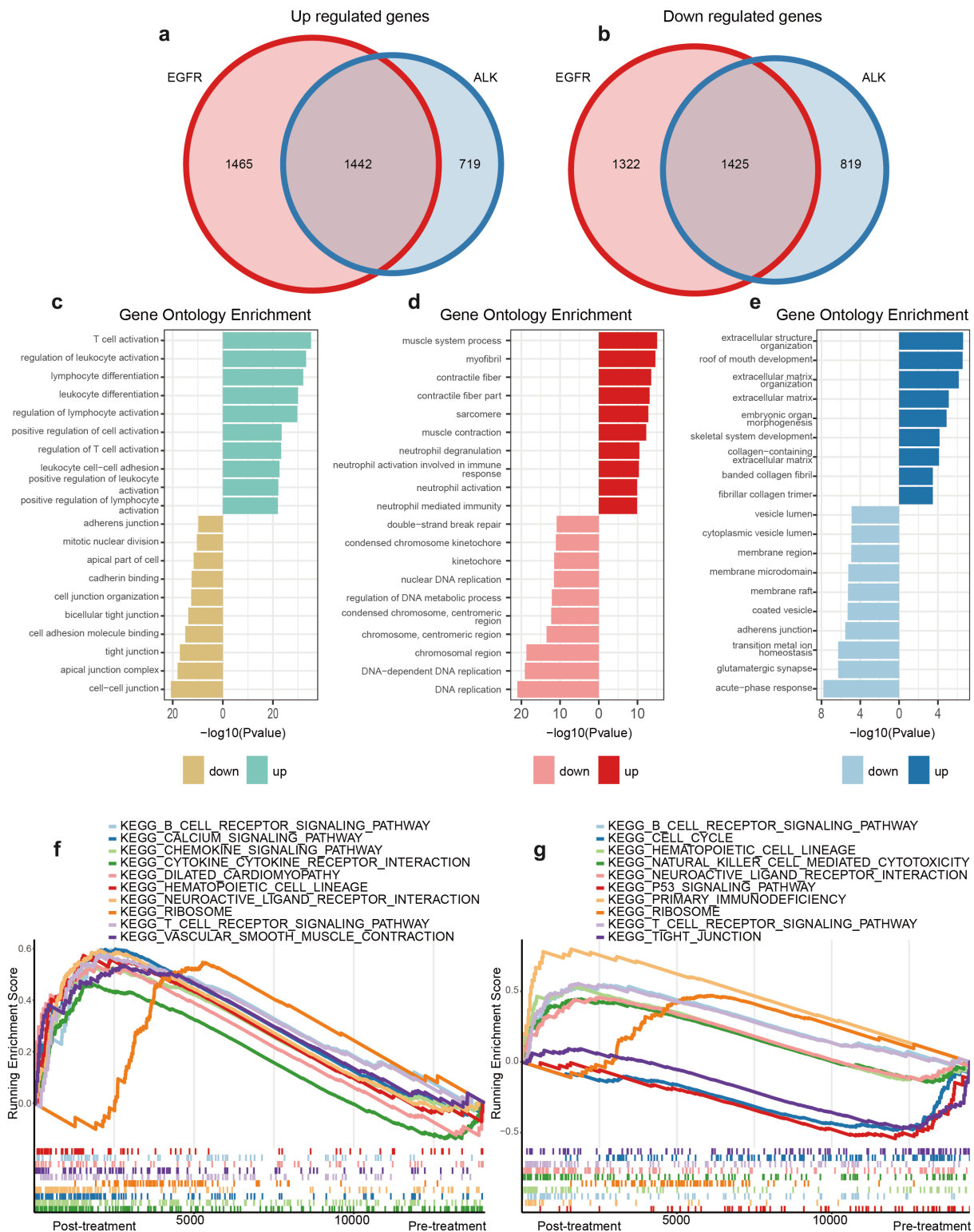


Figure 1. The transcriptional landscape of NSCLCs with EGFR mutations or ALK rearrangements in response to TKI treatments. (a and b) Venn diagram of TKI-induced up-regulated (a) or down-regulated (b) DEGs in EGFR-mutant or ALK-rearranged tissues. (c, d, and e) Representative enriched GO biological process of DEGs shared in EGFR-mutant and ALK-rearranged samples (c) and DEGs unique to EGFR-mutant (d) or ALK-rearranged (e) samples in response to TKI treatments. (f and g) Representative GSEA KEGG pathways in samples with EGFR mutations (f) or ALK rearrangements (g) in response to TKI treatments.

of NEFH.²⁷ A previous study established that NEFH is a cancer driver because of its functional impact on KRAS and MTORC1 signaling.²⁸ We conducted survival analyses of LUAD patients with the EGFR 19Del/L858R mutation or EML4-ALK fusion in the TCGA dataset; our findings suggested that patients with high NEFH expression had worse prognoses than patients with

low NEFH expression (Figure 3(d,e)). Survival analyses of patients with EGFR or ALK mutations in the Pan-Cancer dataset confirmed that NEFH was a cancer-promoting factor (Supplementary Figure 2(a,b)). Consistent with our hypothesis NEFH mutants with functional limitations with EGFR or ALK mutations in the Pan-Cancer dataset showed better

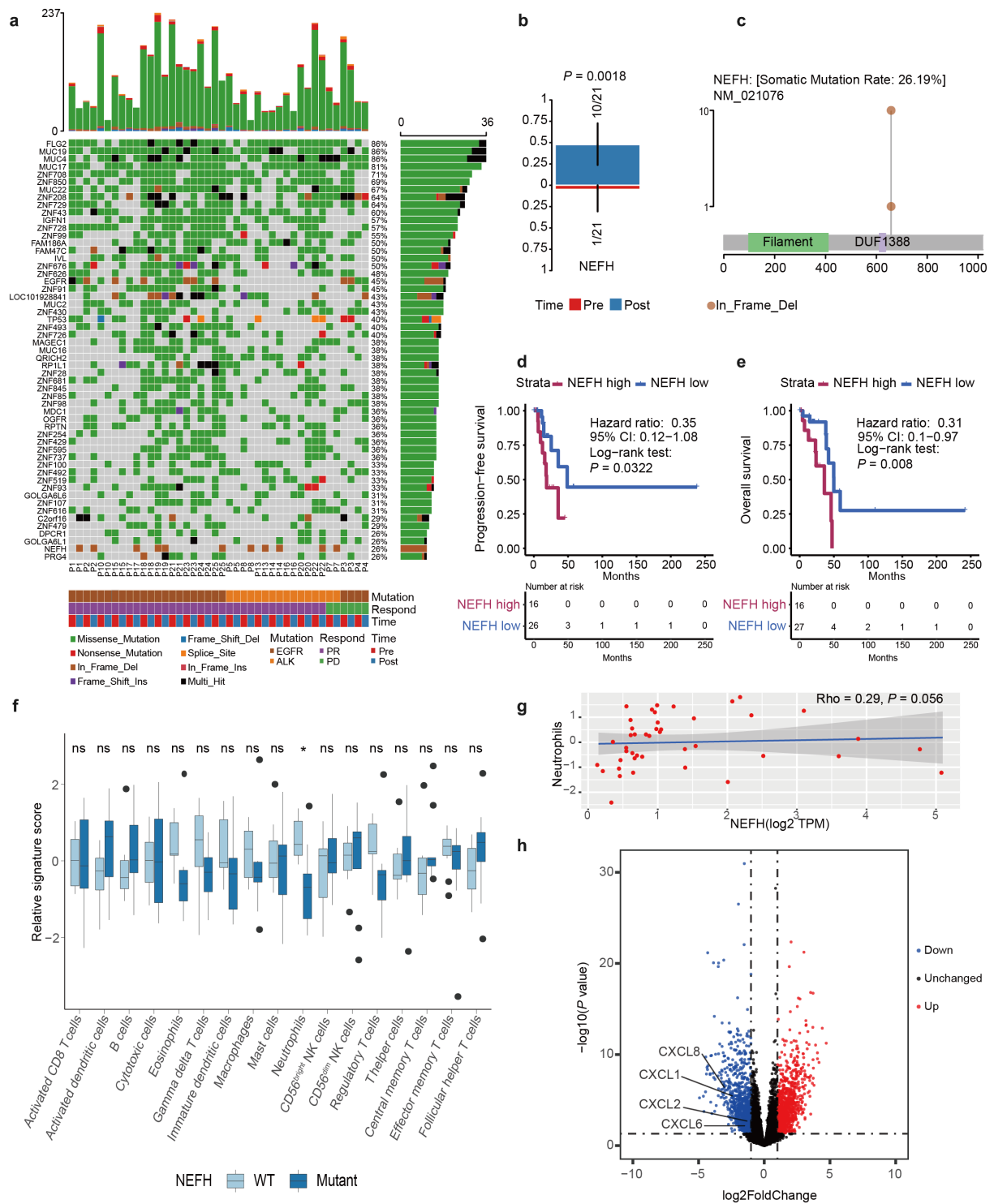


Figure 3. Somatic mutational landscape between pre-treatment and post-treatment samples. (a) OncoPrint of samples before and after TKI treatments, indicating the top-55 genes with the highest mutational frequencies. (b) Differentially enriched mutational genes within samples before and after TKI treatments. (c) Lollipop plot showing the distribution of NEFH mutations across the protein-coding sequence. (d and e) Kaplan-Meier curves of PFS (d) and OS (e) in TCGA LUAD patients with EGFR mutations or ALK rearrangements. The curve was plotted according to $\log_2(\text{NEFH}+1)$ expression with a cutoff of 1.048555. (f) Relative infiltration levels of immune cells in samples that responded after TKI treatments. (g) Spearman's correlation analysis between neutrophil relative abundance and NEFH mRNA expression in TCGA LUAD patients with EGFR mutations or ALK fusion. (h) Volcano plot showing neutrophil-chemotaxis-related DEGs between TKI-naïve and TKI-treated NEFH-mutant samples.

progression-free survival and overall survival than NEFH wild-type patients (Supplementary Figure 2(c,d)).

NEFH mutations are associated with reduced neutrophil infiltration

To investigate the relationship between immunity and NEFH mutations, we calculated the relative infiltration scores of immune cells by subtracting baseline scores before TKI treatment from the scores after TKI treatments. We found that there were lower abundances of neutrophils in NEFH-mutant than in NEFH-wildtype post-treatment samples ($P = .011$; Figure 3(f)), which may aid in inhibiting tumor progression.²⁹ Moreover, Spearman's correlation analysis yielded a positive correlation between NEFH expression and neutrophil infiltration in the TCGA LUAD samples with the EGFR 19Del/L858R mutation or EML4-ALK fusion ($P = .056$, $Rho = 0.29$; Figure 3(g)). Further differential gene expression analysis revealed that the expression of genes related to neutrophil chemotaxis, such as CXCL2 and CXCL8,³⁰ was significantly reduced in NEFH-mutant samples, compared with matched samples before treatment (Figure 3(h)). However, the causal effect of NEFH mutation on neutrophil infiltration needs more research.

Taken together, these findings demonstrate that functionally restricted mutations of NEFH were enriched in samples after rapid TKI-induced responses and may have led to reduced neutrophil infiltration and a better prognosis. However, no significant changes in relative levels of cytotoxic cells were found, which may indicate that NEFH mutations are not the main cause of increased cytotoxic cell infiltration after TKI treatments (Figure 3(f)).

Identification of hub genes involved in TKI-induced immune remodeling via WGCNA

To further explore the mechanisms of TKI-induced cytotoxic cell infiltration, we performed WGCNA to identify relevant intramodular hub genes,³¹ using the top-5000 variation genes in RNA-seq samples to build the co-expression network. This analysis identified nine distinct co-expression modules that corresponded to clusters of correlated genes (Figure 4(a)). Moreover, we analyzed the relationships between the module eigengene and sample clinical characteristics (i.e., pre- vs. post-TKI treatments, immune scores, stroma scores, microenvironment scores, and cytotoxic cell-infiltration scores) to identify co-expression modules associated with the above sample traits. We found that the blue module was strongly positively correlated with TKI treatments, immune scores, microenvironment scores, and cytotoxic cell-infiltration scores, while the turquoise module was negatively associated with TKI treatments and immune scores (Figure 4(b)). Therefore, we focused on the blue and turquoise modules and determined the top-10 genes from each module (Figure 4(c,d)) via the bottleneck method.³² The immune-associated score (IAS) (i.e., mean expression of the hub genes in the blue module minus the mean expression of the hub genes in the turquoise module) was generated (Figure 4(e)). Furthermore, Spearman's correlation analysis confirmed that the immune-associated score had a strong

correlation with cytotoxic-cell infiltration levels, microenvironment scores (Figure 4(f)), and many immune-cell types (Supplementary Figure 3).

Immune-associated score-based subtypes are related to immune infiltration, immune activity, and patient prognosis in the TCGA and GSE11969 cohorts

Next, we validated these hub genes and the IAS in samples with EGFR mutations or ALK fusion in the TCGA LUAD cohort. We found that the IAS was correlated with cytotoxic cell infiltration and immune scores (Figure 5(a,b)). Further analysis confirmed that there was a strong positive correlation between the IAS and many immune cell types (e.g., activated CD8 + T cells) in the TIM (Supplementary Figure 4). Previous studies have demonstrated that there is a direct link between an activated immune microenvironment and favorable clinical outcomes in patients with various forms of cancer.^{33,34} To evaluate the prognostic value of the IAS, we performed Kaplan–Meier curves and smooth hazard ratio (HR) curves of progression-free survival (PFS) and overall survival (OS) of EGFR/ALK-positive patients in the TCGA LUAD cohort. Kaplan–Meier curves showed that under the optimal cutoff point, the high-score group had a higher PFS and OS compared to those of the low-score group (Figure 5(c,d)). Similarly, the analysis of patients with EGFR mutations in the GSE11969 dataset showed that the IAS was significantly associated with the immune remodeling process and patient OS (Figure 5(e,f)).

Discussion

NSCLCs with EGFR mutations or ALK rearrangements are generally inactive tumors with a low tumor mutational burden (TMB)³⁵ and a lack of T-cell infiltration.⁴ Immunotherapy with immune-checkpoint inhibitors has been approved as a treatment for NSCLC.³⁶ It is unlikely that any single immunotherapy will be capable of changing the outcomes of NSCLCs harboring EGFR mutations or ALK rearrangements.^{6,37,38} Although there have been many clinical trials attempting to explore a combination of TKIs and immunotherapy, the results have shown that the clinical benefit is far lower than expected.^{5,39} At present, the data supporting the front-line use of these drugs in EGFR-mutant PD-L1-positive NSCLC patients have been encouraging, but few studies have provided conclusive evidence supporting the combination of TKIs and immunotherapy as front-line treatment for these patients.⁴⁰ Since immune status has a key impact on the efficacy of immunotherapy, further elucidation of the effects of TKI treatments on the immune microenvironment is needed. Unfortunately, previous studies have shown that after the development of TKI resistance, TKI cannot effectively improve T-cell infiltration,^{14,15} and there is a lack of research on the remodeling of the TIM in post-TKI-responsive samples.

In the present study, compared with baseline parameters, TKI treatments significantly improved immune-cell infiltration and cytotoxicity in TKI-responsive samples but not in TKI-resistant samples, which suggests that the combined application of immune-checkpoint inhibitors may be more effective before TKI resistance. Previous studies have shown that the

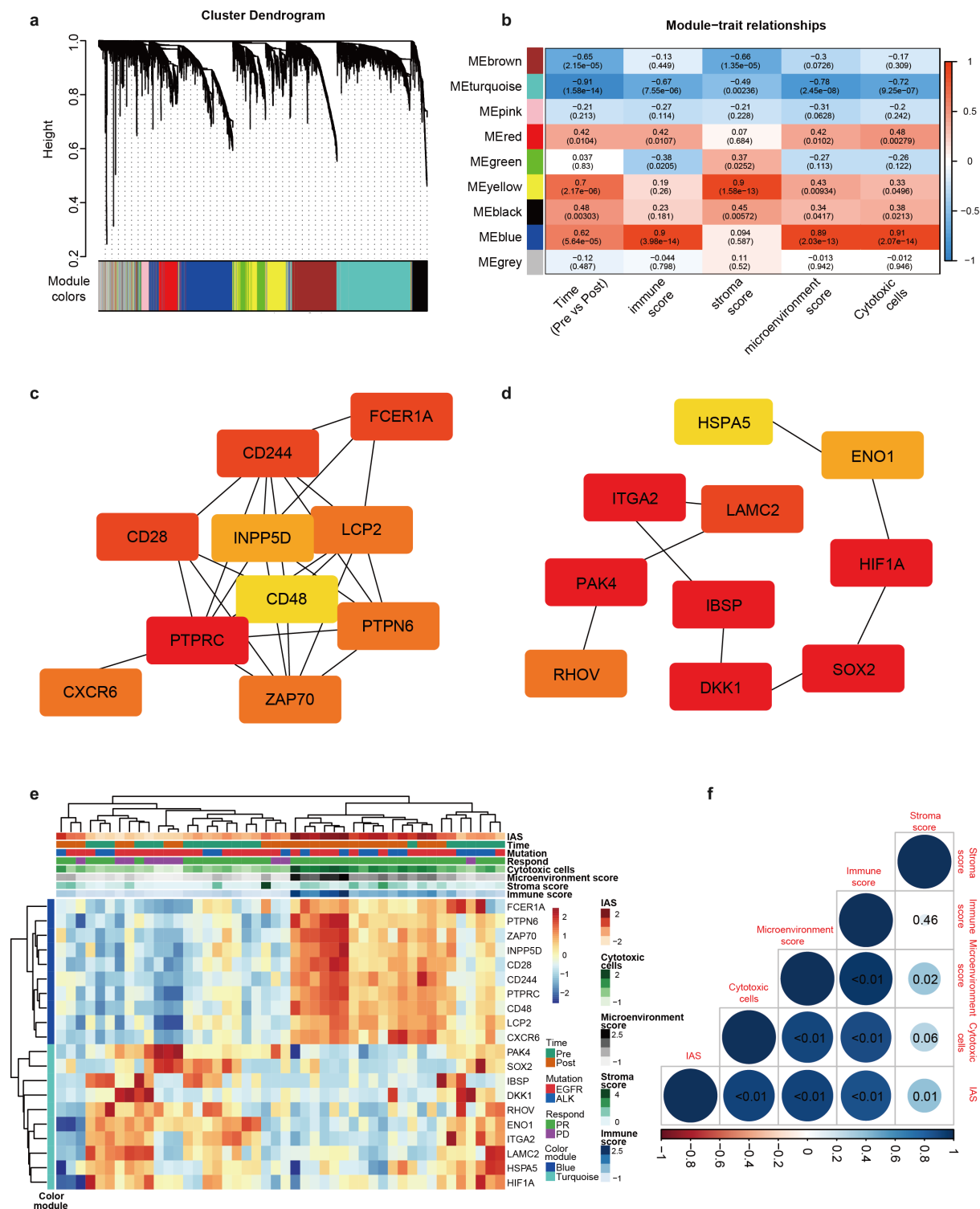


Figure 4. WGCNA-identified hub genes involved in TKI-induced immune remodeling. (a) Dendrogram generated by WGCNA and identification of nine distinct gene modules. (b) Pearson's correlation coefficient matrix between module eigengenes and clinical traits. Accompanied by the corresponding *p*-values in parentheses, the coefficient values range from -1 to 1 depending on the strength of the relationship. (c and d) The networks of hub genes in the blue (c) and turquoise (d) modules. (e) Heatmap of hub-gene expression. (f) Spearman's correlation between the immune-associated score and microenvironment, immune, stroma, and cytotoxic cell scores. The number in each circle represents the *p*-value, and the intensity of the color represents the strength of the correlation.

lower expression level of PD-L1 in EGFR-mutant NSCLCs results in poor inferior response to PD-1/L1 blockade.^{4,7} In our study, TKI treatment did not increase the expression of CD274 (the gene encoding PD-L1 protein), suggesting that the combination of TKI and anti-PD-L1 may not have a significant synergistic effect on tumor treatment. However, a variety of

genes associated with IFN-gamma signaling and immune-checkpoint processes were up-regulated in response to TKI treatments. Further analysis revealed that PDCD1 (the gene encoding PD-1 protein) and other inhibitory-checkpoint genes (e.g., BTLA) were up-regulated following TKI treatments. This finding may explain the poor effects of PD-1 inhibitors

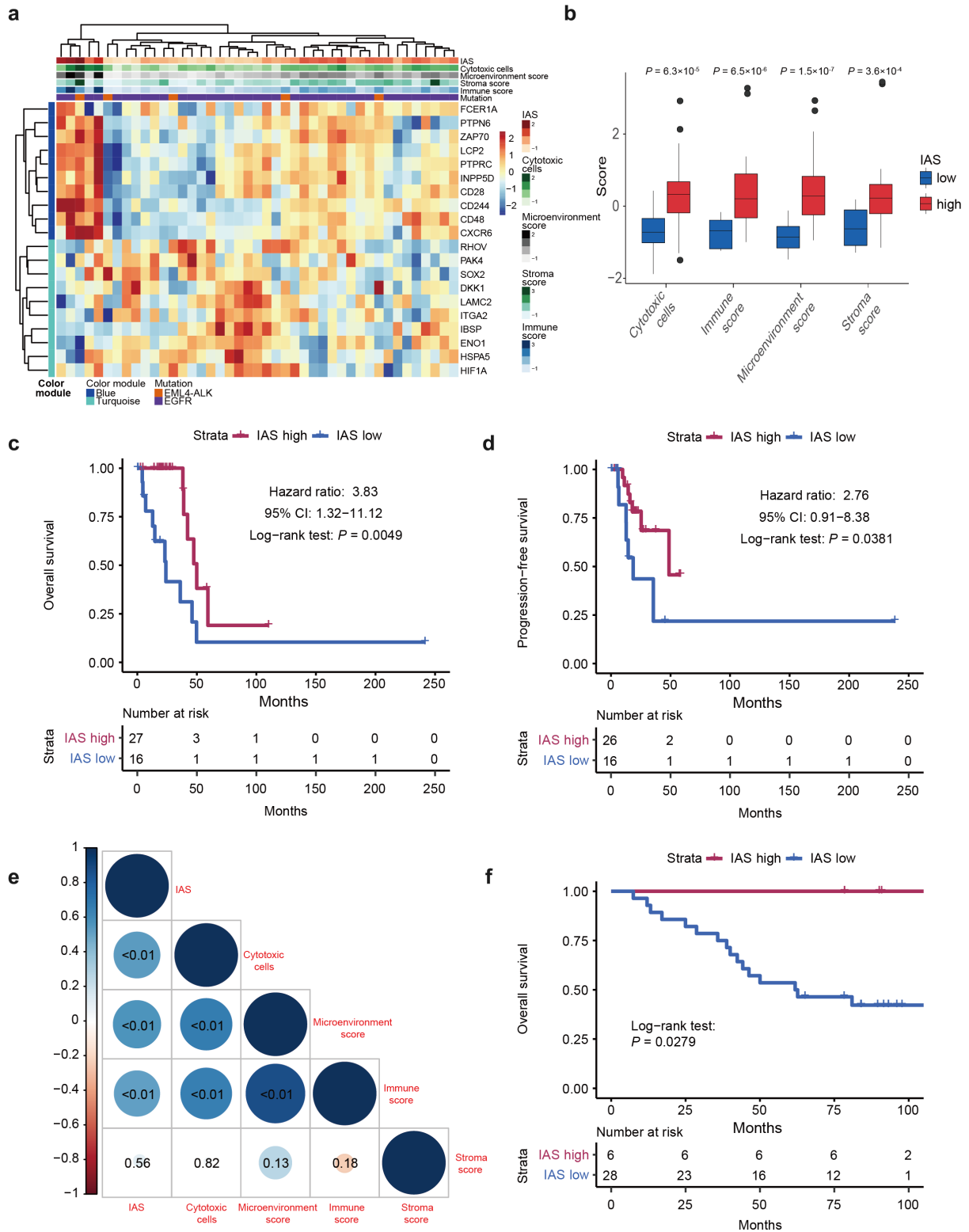


Figure 5. Immune-associated score-based subtypes are related to immune infiltration, immune activity, and patient prognosis in the TCGA and GSE11969 cohorts. (a) Heatmap of hub-gene expression in the TCGA LUAD cohorts with EGFR mutations or ALK rearrangements. (b) Immune scores, microenvironment scores, stroma scores, and cytotoxic-cell scores in the high and low IAS groups from TCGA LUAD patients with EGFR mutations or ALK rearrangements. (c and d) Kaplan–Meier curves of OS (c) and PFS (d) in TCGA LUAD patients with EGFR mutations or ALK rearrangements are shown with optimal cutoff values. (e) Spearman’s correlation between the immune-associated score and microenvironment, immune, stroma, and cytotoxic-cell scores of samples with EGFR mutations from the GSE11969 cohort. The number in each circle represents the *p*-value, and the intensity of the color represents the strength of the correlation. (f) Kaplan–Meier curve of OS in the GSE11969 cohort with EGFR mutations is shown with optimal cutoff values. A cutoff of 0.4821692 (b, c, and d) or 0.305348 (f) was used to distinguish high- and low-score subtypes based on the IAS.

combined with TKIs (immune suppression of multiple immune checkpoints) and may provide evidence for targeting subsequent combination therapies. Furthermore, in ALK post-response samples in the present study, the reduction of antigen-presentation-related genes (e.g., CALR, CANX, and PDIA3), tumor neoantigens, and mutational load may have limited the activation of antigen-specific immune cells such as CD8 + T cells.

Since changes in the genome may also affect immune-cell infiltration, we determined that oncogene NEFH mutations that may have restricted functions were enriched in TKI-treated samples, as determined via WES analysis. We found that NEFH mutations were related to a good prognosis and decreased neutrophils, but were not related to increased cytotoxicity. The complexity of the genomic landscape of EGFR-mutant LUADs was unexpected, and many co-driver gene mutations such as TP53 were related to a poor prognosis.⁴¹ We tried to determine the relationship between TP53 mutation and the changes in TIM after TKI treatment. Surprisingly, we found that the increase in cytotoxicity of EGFR-mutant LUADs with TP53 co-mutation was more significant than that of patients with TP53 wildtype in response to TKI (Supplementary Figure 5(a)), which may have resulted from the loss of immunosuppressive TP53 co-mutation after TKI treatment.⁴² However, the more obvious cytotoxicity up-regulation was found in ALK-rearranged LUAD with TP53 wildtype (Supplementary Figure 5(b)). These findings revealed that TP53 mutation may be a predictor of the effectiveness of TKI-immunotherapy combinations for NSCLCs, but further studies are needed.

Next, we identified hub genes related to the TKI-induced increase in immune infiltration via WGCNA and the bottleneck method, from which we determined the IAS. Interestingly, we found that the IAS composed of the hub genes driven by TKI-induced immune remodeling was positively correlated with immune infiltration. Based on the IAS, we divided the samples of the public dataset into high-score and low-score groups, and these two groups of samples showed differential prognoses and immune infiltration patterns, the findings of which deserve further investigation.

Taken together, we revealed the complexity of TKI-induced immune remodeling in TKI-responsive samples with EGFR mutations or ALK rearrangements, in which changes in immune-related mRNA and NEFH mutations may also play an important role. Nevertheless, the present study has a limitation of not fully considering the issue of intratumoral heterogeneity, which was reported to be a potential cause for the difference in response to TKI.^{41,43} Moreover, the relationship between TIM and TKI should be validated by using a large-sized sample and some other *in vitro* or *in vivo* experimental studies. Despite these limitations, the present study provides clues for combination therapy of TKI and immunotherapy.

Acknowledgments

The authors would like to thank Nanjing Geneseq Technology Inc. for providing help with data analysis.

Disclosure Statement

No potential conflicts of interest were disclosed.

Funding

This work was supported by the Science and Technology Planning Project of Guangdong Province [Grant Number: 2020A0505090007] and The Science and Technology Planning Project of Guangzhou, China [Grant Number: 201804010019].

ORCID

Wangjun Liao  <http://orcid.org/0000-0002-1364-8442>

Author contributions

W.J.L. designed and directed the study. Y.S.F., Y.Y.W., and D.Q.Z. collected clinical specimens of patients, analyzed the data, and wrote the manuscript. S.M.Z. and T.T.S. collected blood and tumor samples and conducted the experiment. N.H., S.T.Z., J.H.W. and Y.T.L. performed the experimental work and organized the public data. G.J.H. and Y.C.X. took charge of data visualization and statistical analysis. J.P.B., Y.L.L., and M.S. revised and edited the manuscript. All authors have read and approved the final version.

References

1. Yang C-Y, Yang JC-H, Yang P-C. Precision management of advanced non-small cell lung cancer. *Annu Rev Med.* 2020;71(1):117–136. doi:10.1146/annurev-med-051718-013524.
2. Rotow J, Bivona TG. Understanding and targeting resistance mechanisms in NSCLC. *Nat Rev Cancer.* 2017;17(11):637–658. doi:10.1038/nrc.2017.84.
3. Feliciano P. Acquired resistance in lung cancer. *Nat Genet.* 2012;44(3):241. doi:10.1038/ng.2209.
4. Gainor JF, Shaw AT, Sequist LV, Fu X, Azzoli CG, Piotrowska Z, Huynh TG, Zhao L, Fulton L, Schultz KR, et al. EGFR mutations and ALK rearrangements are associated with low response rates to PD-1 pathway blockade in non-small cell lung cancer: a retrospective analysis. *Clin Cancer Res.* 2016;22(18):4585–4593. doi:10.1158/1078-0432.CCR-15-3101.
5. Spigel DR, Reynolds C, Waterhouse D, Garon EB, Chandler J, Babu S, Thurmes P, Spira A, Jotte R, Zhu J, et al. Phase 1/2 study of the safety and tolerability of nivolumab plus crizotinib for the first-line treatment of anaplastic lymphoma kinase translocation — positive advanced non-small cell lung cancer (CheckMate 370). *J Thorac Oncol.* 2018;13(5):682–688. doi:10.1016/j.jtho.2018.02.022.
6. Garassino MC, Cho BC, Kim JH, Mazières J, Vansteenkiste J, Lena H, Corral Jaime J, Gray JE, Powderly J, Chouaid C, et al. Durvalumab as third-line or later treatment for advanced non-small-cell lung cancer (ATLANTIC): an open-label, single-arm, phase 2 study. *Lancet Oncol.* 2018;19(4):521–536. doi:10.1016/S1470-2045(18)30144-X.
7. Dong Z-Y, Zhang J-T, Liu S-Y, Su J, Zhang C, Xie Z, Zhou Q, Tu H-Y, Xu C-R, Yan L-X, et al. EGFR mutation correlates with uninfamed phenotype and weak immunogenicity, causing impaired response to PD-1 blockade in non-small cell lung cancer. *Oncoimmunology.* 2017;6(11):e1356145. doi:10.1080/2162402X.2017.1356145.
8. Ota K, Azuma K, Kawahara A, Hattori S, Iwama E, Tanizaki J, Harada T, Matsumoto K, Takayama K, Takamori S, et al. Induction of PD-L1 expression by the EML4-ALK oncoprotein and down stream signaling pathways in non-small cell lung cancer. *Clin Cancer Res.* 2015;21(17):4014–4021. doi:10.1158/1078-0432.CCR-15-0016.

9. Koh J, Jang JY, Keam B, Kim S, Kim MY, Go H, Kim TM, Kim DW, Kim CW, Jeon YK, et al. EML4-ALK enhances programmed cell death-ligand 1 expression in pulmonary adenocarcinoma via hypoxia-inducible factor (HIF)-1 α and STAT3. *Oncoimmunology*. 2016;5(3):1–13. doi:10.1080/2162402X.2015.1108514.
10. Chen N, Fang W, Zhan J, Hong S, Tang Y, Kang S, Zhang Y, He X, Zhou T, Qin T, et al. Upregulation of PD-L1 by EGFR activation mediates the immune escape in EGFR-driven NSCLC: implication for optional immune targeted therapy for NSCLC patients with EGFR mutation. *J Thorac Oncol*. 2015;10(6):910–923. doi:10.1097/JTO.0000000000000500.
11. Hong S, Chen N, Fang W, Zhan J, Liu Q, Kang S, He X, Liu L, Zhou T, Huang J, et al. Upregulation of PD-L1 by EML4-ALK fusion protein mediates the immune escape in ALK positive NSCLC: implication for optional anti-PD-1/PD-L1 immune therapy for ALK-TKIs sensitive and resistant NSCLC patients. *Oncoimmunology*. 2016;5(3):1–12. doi:10.1080/2162402X.2015.1094598.
12. Liu P, Zhao L, Pol J, Levesque S, Petrazzuolo A, Pfirschke C, Engblom C, Rickelt S, Yamazaki T, Iribarren K, et al. Crizotinib-induced immunogenic cell death in non-small cell lung cancer. *Nat Commun*. 2019;10(1). doi:10.1038/s41467-019-09415-3.
13. Pozzi C, Cuomo A, Spadoni E, Magni E, Silvola A, Conte A, Sigismund S, Ravenda PS, Bonaldi T, Zampino MG, et al. The EGFR-specific antibody cetuximab combined with chemotherapy triggers immunogenic cell death. *Nat Med*. 2016;22(6):624–631. doi:10.1038/nm.4078.
14. Isomoto K, Haratani K, Hayashi H, Shimizu S, Tomida S, Niwa T, Yokoyama T, Fukuda Y, Chiba Y, Kato R, et al. Impact of EGFR-TKI treatment on the tumor immune microenvironment in EGFR mutation-positive non-small cell lung cancer. *Clin Cancer Res*. 2020;26(8):2037–2046. doi:10.1158/1078-0432.CCR-19-2027.
15. Pyo KH, Lim SM, Park CW, Jo HN, Kim JH, Yun MR, Kim D, Xin CF, Lee W, Gheorghiu B, et al. Comprehensive analyses of immunodynamics and immunoreactivity in response to treatment in ALK-positive non-small-cell lung cancer. *J Immunother Cancer*. 2020;8(2). doi:10.1136/jitc-2020-000970.
16. Roper N, Brown A-L, Wei JS, Pack S, Trindade C, Kim C, Restifo O, Gao S, Sindiri S, Mehrabadi F, et al. Clonal evolution and heterogeneity of osimertinib acquired resistance mechanisms in EGFR mutant lung cancer. *Cell Rep Med*. 2020;1(1):100007. doi:10.1016/j.xcrm.2020.100007.
17. Eisenhauer EA, Therasse P, Bogaerts J, Schwartz LH, Sargent D, Ford R, Dancey J, Arbuck S, Gwyther S, Mooney M, et al. New response evaluation criteria in solid tumours: revised RECIST guideline (version 1.1). *Eur J Cancer*. 2009;45(2):228–247. doi:10.1016/j.ejca.2008.10.026.
18. Yu G, Wang LG, Han Y, He QY. ClusterProfiler: an R package for comparing biological themes among gene clusters. *Omi J Integ Biol*. 2012;16(5):284–287. doi:10.1089/omi.2011.0118.
19. Tamborero D, Rubio-Perez C, Muiños F, Sabarinathan R, Piulats JM, Muntasell A, Dienstmann R, Lopez-Bigas N, Gonzalez-Perez A. A pan-cancer landscape of interactions between solid tumors and infiltrating immune cell populations. *Clin Cancer Res*. 2018;24(15):3717–3728. doi:10.1158/1078-0432.CCR-17-3509.
20. Hänzelmann S, Castelo R, Guinney J. GSEA: gene set variation analysis for microarray and RNA-Seq data. *BMC Bioinform*. 2013;14. doi:10.1186/1471-2105-14-7.
21. Aran D, Hu Z, Butte AJ. xCell: digitally portraying the tissue cellular heterogeneity landscape. *Genome Biol*. 2017;18(1):1–14. doi:10.1186/s13059-017-1349-1.
22. Yoshihara K, Shahmoradgoli M, Martínez E, Vegesna R, Kim H, Torres-García W, Treviño V, Shen H, Laird PW, Levine DA, et al. Inferring tumour purity and stromal and immune cell admixture from expression data. *Nat Commun*. 2013;4. doi:10.1038/ncomms3612.
23. Abel AM, Yang C, Thakar MS, Malarkannan S. Natural killer cells: development, maturation, and clinical utilization. *Front Immunol*. 2018;9(AUG):1–23. doi:10.3389/fimmu.2018.01869.
24. Leone P, Shin EC, Perosa F, Vacca A, Dammacco F, Racanelli V. MHC class I antigen processing and presenting machinery: organization, function, and defects in tumor cells. *J Natl Cancer Inst*. 2013;105(16):1172–1187. doi:10.1093/jnci/djt184.
25. Smith CC, Selitsky SR, Chai S, Armistead PM, Vincent BG, Serody JS. Alternative tumour-specific antigens. *Nat Rev Cancer*. 2019;19(8):465–478. doi:10.1038/s41568-019-0162-4.
26. Hallberg B, Palmer RH. Mechanistic insight into ALK receptor tyrosine kinase in human cancer biology. *Nat Rev Cancer*. 2013;13(10):685–700. doi:10.1038/nrc3580.
27. Rooke K, Figlewicz DA, Han F-Y, Rouleau GA. Analysis of the KSP repeat of the neurofilament heavy subunit in familial amyotrophic lateral sclerosis. *Neurology*. 1996;46(3):789–790. doi:10.1212/WNL.46.3.789.
28. Cai C, Cooper GF, Lu KN, Ma X, Xu S, Zhao Z, Chen X, Xue Y, Lee AV, Clark N, et al. Systematic discovery of the functional impact of somatic genome alterations in individual tumors through tumor-specific causal inference. *bioRxiv*. 2018;1–29. doi:10.1101/329375.
29. Kargl J, Busch SE, Yang GHY, Kim KH, Hanke ML, Metz HE, Hubbard JJ, Lee SM, Madtes DK, McIntosh MW, et al. Neutrophils dominate the immune cell composition in non-small cell lung cancer. *Nat Commun*. 2017;8:1–11. doi:10.1038/ncomms14381.
30. Jaillon S, Ponzetta A, Di Mitri D, Santoni A, Bonecchi R, Mantovani A. Neutrophil diversity and plasticity in tumour progression and therapy. *Nat Rev Cancer*. 2020;20(9):485–503. doi:10.1038/s41568-020-0281-y.
31. Langfelder P, Horvath S. WGCNA: an R package for weighted correlation network analysis. *BMC Bioinform*. 2008;9. doi:10.1186/1471-2105-9-559.
32. Yu H, Kim PM, Sprecher E, Trifonov V, Gerstein M. The importance of bottlenecks in protein networks: correlation with gene essentiality and expression dynamics. *PLoS Comput Biol*. 2007;3(4):713–720. doi:10.1371/journal.pcbi.0030059.
33. Fridman WH, Zitvogel L, Sautès-Fridman C, Kroemer G. The immune contexture in cancer prognosis and treatment. *Nat Rev Clin Oncol*. 2017;14(12):717–734. doi:10.1038/nrclinonc.2017.101.
34. Bruni D, Angell HK, Galon J. The immune contexture and Immunoscore in cancer prognosis and therapeutic efficacy. *Nat Rev Cancer*. 2020. doi:10.1038/s41568-020-0285-7.
35. Spigel DR, Schrock AB, Fabrizio D, Frampton GM, Sun J, He J, Gowen K, Johnson ML, Bauer TM, Kalemkerian GP, et al. Total mutation burden (TMB) in lung cancer (LC) and relationship with response to PD-1/PD-L1 targeted therapies. *J Clin Oncol*. 2016;34(15_suppl):9017–9017. doi:10.1200/jco.2016.34.15_suppl.9017.
36. Mezquita L, Auclin E, Ferrara R, Charrier M, Remon J, Planchard D, Ponce S, Ares LP, Leroy L, Audigier-Valette C, et al. Association of the lung immune prognostic index with immune checkpoint inhibitor outcomes in patients with advanced non-small cell lung cancer. *JAMA Oncol*. 2018;4(3):351–357. doi:10.1001/jamaoncol.2017.4771.
37. Lisberg A, Cummings A, Goldman JW, Bornazyan K, Reese N, Wang T, Coluzzi P, Ledezma B, Mendenhall M, Hunt J, et al. A phase II study of pembrolizumab in EGFR-mutant, PD-L1+, tyrosine kinase inhibitor naïve patients with advanced NSCLC. *J Thorac Oncol*. 2018;13(8):1138–1145. doi:10.1016/j.jtho.2018.03.035.
38. Mazieres J, Drilon A, Lusque A, Mhanna L, Cortot AB, Mezquita L, Thai AA, Mascaux C, Couraud S, Veillon R, et al. Immune checkpoint inhibitors for patients with advanced lung cancer and oncogenic driver alterations: results from the IMMUNOTARGET registry. *Ann Oncol*. 2019;30(8):1321–1328. doi:10.1093/annonc/mdz167.
39. Chih-Hsin Yang J, Shepherd FA, Kim DW, Lee GW, Lee JS, Chang GC, Lee SS, Wei YF, Lee YG, Laus G, et al. Osimertinib plus durvalumab versus osimertinib monotherapy in EGFR T790M-positive NSCLC following previous EGFR TKI therapy: CAURAL brief report. *J Thorac Oncol*. 2019;14(5):933–939. doi:10.1016/j.jtho.2019.02.001.

40. D'Incecco A, Andreozzi M, Ludovini V, Rossi E, Capodanno A, Landi L, Tibaldi C, Minuti G, Salvini J, Coppi E, et al. PD-1 and PD-L1 expression in molecularly selected non-small-cell lung cancer patients. *Br J Cancer*. 2015;112(1):95–102. doi:10.1038/bjc.2014.555.
41. Nahar R, Zhai W, Zhang T, Takano A, Khng AJ, Lee YY, Liu X, Lim CH, Koh TPT, Aung ZW, et al. Elucidating the genomic architecture of Asian EGFR-mutant lung adenocarcinoma through multi-region exome sequencing. *Nat Commun*. 2018;9(1). doi:10.1038/s41467-017-02584-z.
42. Muñoz-Fontela C, Mandinova A, Aaronson SA, Lee SW. Emerging roles of p53 and other tumour-suppressor genes in immune regulation. *Nat Rev Immunol*. 2016;16(12):741–750. doi:10.1038/nri.2016.99.
43. Guo L, Chen Z, Xu C, Zhang X, Yan H, Su J, Yang J, Xie Z, Guo W, Li F, et al. Intratumoral heterogeneity of EGFR-activating mutations in advanced NSCLC patients at the single-cell level. *BMC Cancer*. 2019;19(1):1–8. doi:10.1186/s12885-019-5555-y.